Measurement of the absolute timing of attosecond XUV bursts with respect to the driving field

doi: 10.1103/PhysRevA.85.051802

PHYSICAL REVIEW A **85**, 051802(R) (2012)

Measurement of the absolute timing of attosecond XUV bursts with respect to the driving field

Niranjan Shivaram,[1,*] Henry Timmers,[1] Xiao-Min Tong,[2] and Arvinder Sandhu[1,†]
[1]*Department of Physics, University of Arizona, Tucson, Arizona 85721, USA*
[2]*Center for Computational Sciences, University of Tsukuba, Ibaraki 305-8573, Japan*
(Received 8 November 2011; published 14 May 2012)

We demonstrate that a simple two-color ionization measurement can be used to extract the time of birth of attosecond extreme ultraviolet pulses. A high-order-harmonic attosecond pulse train generated in xenon gas is used to excite a laser-dressed helium atom, which we model using the Floquet formalism. The interference between ionization paths from different Fourier components of the Floquet states results in the oscillation of ion yield with time delay. Using two IR pulses to create a reference intensity modulation, we obtain the phase of ion-yield oscillations, which provides the absolute timing of attosecond bursts with respect to the driving IR field.

DOI: 10.1103/PhysRevA.85.051802 PACS number(s): 42.65.Ky, 32.80.Fb

The discovery of laser high-order-harmonic generation (HHG) process seeded a revolution in the field of atomic and molecular sciences [1]. The dynamics of electrons in strong fields and the process of high-order-harmonic generation still represent active fields of investigation. Recently, the HHG process itself has been used as a probe of atomic wave functions [2] and multielectron dynamics [3]. One important use of the HHG process is in the generation of attosecond pulse trains (APT) and single attosecond pulses approaching durations shorter than 100 as [1,4–7]. These extreme-ultraviolet (XUV) attosecond sources allow direct probing of fast electron dynamics in atoms, molecules, and materials through photoionization and photoexcitation mechanisms.

Due to the importance of attosecond sources in cutting-edge investigations of atomic and molecular processes, it is very important to have robust methods for characterizing the spectral and temporal nature of these sources [4,8,9]. The spectral content of attosecond bursts is often fairly easy to obtain, but the measurement of temporal structure is nontrivial and requires precision, pump-probe measurements of electron spectra. For temporal characterization of single attosecond pulses, streaking methods have been used [8]. In the case of attosecond pulse trains, XUV pulse autocorrelation [9] and the reconstruction of attosecond beating by interference of two-photon transitions (RABBITT) techniques [4,10] have been utilized. In the RABBITT approach, attosecond XUV bursts are converted to continuum electron wave packets through ionization of atoms in the presence of moderate strength visible or near-infrared (IR) laser fields. The interference between two-photon continuum transitions modulates the electronic yield at a specific phase. Knowing this phase as a function of energy allows characterization of the temporal profile of attosecond bursts [4]. In such measurements, the absolute timing of attosecond pulses relative to the driving field is not directly accessible. However, variations of the RABBITT method can be used to obtain the timing information [11,12]. Here, we demonstrate another straightforward method that provides the absolute timing of attosecond bursts directly from ion-yield measurements in XUV + IR photoionization of helium. One major simplification in our method is that it is purely based on ion counting and there is no requirement of energy-resolved measurements of electrons.

In our experimental setup, an amplified 65-fs, 785-nm IR pulse of 1.5-mJ energy is split into two pulses using a broadband beam splitter. One pulse of intensity $\sim 6 \times 10^{13}$ W cm^{-2} is focused onto a xenon gas-filled hollow-glass waveguide to generate high-order harmonics in the form of an APT. The APT along with the copropagating HHG-driver beam (IR$_d$) is focused onto an effusive helium gas jet using a toroidal mirror. The copropagating IR pulse (IR$_d$) is phase locked to the APT due to the mechanism of generation and has an intensity of $\sim 3 \times 10^{10}$ W cm^{-2} in the interaction region. The second pulse (IR$_p$) goes to a precision delay stage and is then focused with a 50 cm lens onto the He target in the interaction region with a peak intensity $\sim 3 \times 10^{12}$ W cm^{-2}. In the interaction region, the XUV and IR fields are linearly polarized along the z direction. Additional experimental details can be found in an earlier publication [13]. The He^+ ions are imaged using a spatially selective Gouy phase gating technique which allows us to eliminate Gouy phase averaging and obtain a high-quality signal [13].

Figure 1(a) shows the configuration of the pulses used in the experiment and defines the sign conventions used in the theoretical model discussed below. Figure 1(b) shows the harmonic spectra generated in Xe. There are only two dominant harmonics (13th and 15th) in the XUV spectrum. These harmonics are located near the field-free $2p$, $4p$, and $5p$ atomic resonances. Under the action of a strong femtosecond IR pulse, the He atomic structure substantially changes with time, and the ionization pathways evolve dynamically [14]. We will utilize the ion-yield measurements under these dynamic conditions to extract the timing of attosecond bursts relative to the driving IR field.

The XUV APT creates excited states in helium which were simultaneously modified and ionized by an IR field created by the superposition of two pulses, the driver (IR$_d$) and the probe (IR$_p$). In this configuration [Fig. 1(a)] where the APT + IR$_d$ is delayed with respect to the probe IR (IR$_p$), the electric fields for IR$_p$, IR$_d$, and net IR can be written,

*niranjan@physics.arizona.edu
†sandhu@physics.arizona.edu

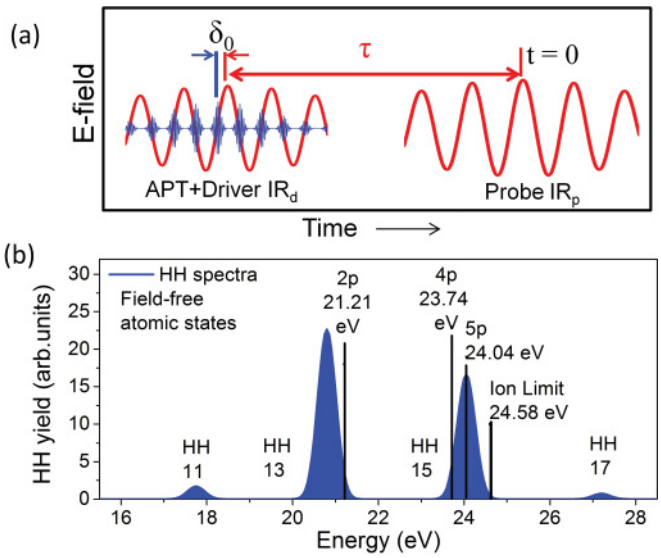

FIG. 1. (Color online) (a) The configuration of the APT, IR_d, and IR_p used in the experiment. The APT is inherently phase locked to the driver IR_d at a phase δ_0, which we are interested in measuring. Our sign conventions are such that time delay τ is positive when IR_d arrives earlier in time and δ_0 is positive when the attosecond bursts are located earlier than the peak of IR_d cycle. (b) The XUV spectrum used in the experiment and the relevant He atomic states.

respectively, as

$$E_p = A_p \cos(\omega t),$$
$$E_d = A_d \cos(\omega t + \omega\tau),$$
$$E_{\text{net}} = \sqrt{I(\tau)}\cos[\omega t + \delta(\tau)],$$

where

$$I(\tau) = A_p^2 + A_d^2 + 2A_pA_d\cos(\omega\tau)$$

and

$$\delta(\tau) = \arcsin[A_d \sin(\omega\tau)/\sqrt{I(\tau)}],$$

where ω is the angular frequency of the IR fields.

The XUV field in the time domain can be written as an inverse Fourier transform of the high-order-harmonic field in the frequency domain as

$$E_X = \int f(\omega_x)e^{-i\omega_x(t+\tau+\delta_0/\omega)}\,d\omega_x, \tag{1}$$

where $f(\omega_x)$ is the harmonic spectral amplitude and δ_0/ω is the time at which the attosecond bursts are locked with respect to the peak of IR_d. This is the time of birth of the attosecond bursts as they come out of the gas-filled capillary in which they are generated. The measurement of δ_0 thus provides the absolute timing of the attosecond pulses.

The high-order harmonics present in the XUV pulse excite an atom from its ground state to laser-dressed atomic states, which can be considered as Floquet states [15,16] for multicycle laser fields. In this picture, each Floquet state is represented by a series of Fourier components that are spaced by the dressing laser frequency ω. The Floquet manifold for the atomic $2p$ state is shown in Fig. 2(a) along with the 13th and 15th harmonics used for excitation in our experiment. Mathematically, the Floquet manifold associated with an atomic state can be written as [15–17]

$$\psi_\alpha(t) = e^{-i\epsilon_\alpha[t+\delta(\tau)/\omega]}\sum_n \phi_{\alpha n}e^{-in\omega[t+\delta(\tau)/\omega]}, \tag{2}$$

where ϵ_α is the quasienergy of the Floquet state and $\phi_{\alpha n}$ is the wave function of the nth Fourier component of this Floquet state.

The photoexcitation probability can be calculated as the XUV dipole matrix element from the ground state to a Floquet state using Eqs. (1) and (2) and integrating over time. We can then write the photoionization probability, which is proportional to the excitation probability, as

$$P(\tau) \propto \left|\sum_n \langle\phi_{\alpha n}|z|\phi_g\rangle f(\omega_n)e^{-in[\omega\tau+\delta_0-\delta(\tau)]}\right|^2, \tag{3}$$

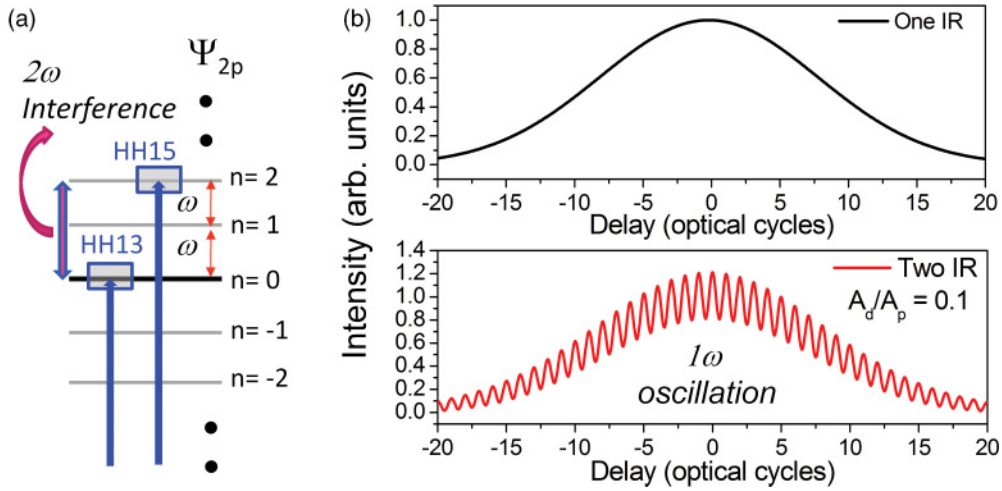

FIG. 2. (Color online) (a) The Floquet manifold corresponding to the $2p$ state and the two harmonics used in our experiment. The interference between two Fourier paths leads to 2ω oscillation. (b) The net IR intensity variation at the timing of the XUV burst for the case of a single IR pulse and two IR pulses. Use of two IR pulses leads to an intensity modulation at ω, which acts as a reference in our experiment.

where ϕ_g is the ground-state wave function and $f(\omega_n)$ is the XUV spectral amplitude Eq. (1) at the energy corresponding to the nth Fourier component of the excited Floquet state.

In our experiment, as we have only two dominant harmonics (13th and 15th) in the XUV spectrum, only two Fourier components of the Floquet state need to be considered, and hence the ionization probability can be simplified as

$$P(\tau) \propto |M_0 f_0 + M_2 f_2 e^{-i[2\omega\tau + 2\delta_0 - 2\delta(\tau) + \phi]}|^2, \quad (4)$$

where M_0 and M_2 are the two transition matrix elements and f_0 and f_2 are the strengths of the two harmonics at the energies corresponding to the $n = 0$ and $n = 2$ components of a given Floquet state [Fig. 2(a)]. The matrix elements depend on the net IR intensity [$I(\tau)$, Fig. 2(b)], which modulates at frequency ω. Importantly, the matrix elements are real and can only be either positive or negative. The relative sign of matrix elements is included in this expression through ϕ, which can take values 0 or π.

We utilize the fact that in our experimental geometry $A_d/A_p \ll 1$ to retain only first-order terms in A_d/A_p. This leads to the following simplified expression for the probability of ionization:

$$P(\tau) = P_1(\tau)\cos(\omega\tau) + P_2(\tau)\cos(2\omega\tau + 2\delta_0 + \phi). \quad (5)$$

$P_1(\tau)$ and $P_2(\tau)$ are the time-delay-dependent amplitudes of the two frequencies in the signal. The phase term δ_0 is, of course, the desired quantity in this Rapid Communication.

The ionization probability given by Eq. (5) exhibits periodic oscillations at ω and 2ω frequencies. The experimental measurements of the He^+ ion yield shown in Fig. 3 also have an oscillation structure with these two frequencies, indicating that our model correctly captures the essence of the XUV + 2IR ionization process. We note that similar 2ω oscillations have also been observed in other experiments [18].

The half-cycle (i.e., 2ω) oscillation in Fig. 3 can be interpreted as a quantum interference between different Fourier components of the Floquet states [16], as illustrated in Fig. 2(a). The one-cycle (i.e., ω) variation is due to interference between two IR fields that leads to a net IR intensity modulation at ω frequency [Fig. 2(b)].

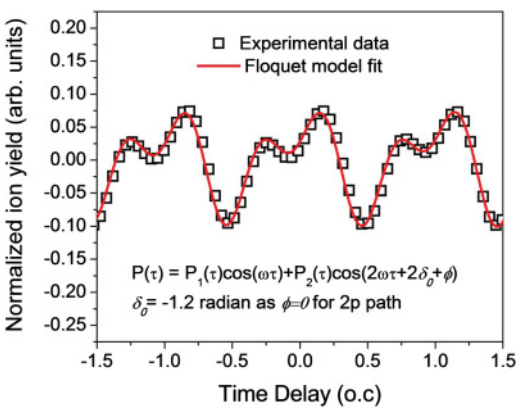

FIG. 3. (Color online) Experimental He^+ ion yield in the presence of XUV and two IR fields as a function of time delay between the APT + IR_d and IR_p. The fit obtained using a model for Floquet interferences in XUV + 2IR fields described by Eq. (5) is also shown.

Before we proceed with further data analysis using our model, it is important to realize that Eq. (5) describes the ionization resulting from a single Floquet state. In contrast, the helium atom has many relevant "np" atomic states, which can all be interpreted in terms of Floquet states in the presence of an IR field. In particular, as Fig. 1(b) shows, the field-free $2p$, $4p$, and $5p$ atomic states are nearly resonant with the 13th and 15th harmonics. However, if ionization contribution from a certain Floquet state is dominant over the others, the total ionization yield can be modeled by Eq. (5) for the dominant state. Since phase terms corresponding to various Floquet states only differ by 0 or π, the phase of the net ionization signal is completely determined by the phase term of the dominant Floquet state.

The 13th and 15th harmonics in our case predominantly excite $2p$, $4p$, and $5p$ states. However, the photoabsorption cross section of these states is strongly dependent on the IR field strength. The modification of the atomic structure in the presence of a strong field is discussed in [19]. Figure 4(a) shows the calculated ionization probability for $2p$, $4p$, and $5p$ states as a function of IR laser intensity. To obtain this plot, we performed time-dependent Schrödinger equation (TDSE) simulations using a method discussed in Ref. [16]. We identified the contribution of $2p$, $4p$, and $5p$ states to the total ionization yield by artificially removing these resonances from the calculation. From the plot, we can see that above an intensity of $\sim 3 \times 10^{12}$ W/cm^2, the ionization from the $2p$ state is the dominant contribution to the total ionization. Figure 4(b) is a schematic of the evolution of the different Floquet blocks with IR intensity which illustrates how the $2p$ state comes into resonance at higher intensities. Since it has more than an order of magnitude higher absorption cross section compared to the $4p$ and $5p$ states, the $2p$ state dominates the absorption and hence the ionization process. In the measurement corresponding to Fig. 3, we used an intensity of 3.4×10^{12} W cm^{-2} at which the $2p$ state clearly dominates.

Since a single Floquet state path corresponding to the atomic $2p$ state dominates the ionization yield, we can obtain the phase term in Eq. (5) from the experimental data. Fourier transforming the experimental data in Fig. 3, we extract the P_1 and P_2 amplitude terms. This leaves only the quantity $\phi + 2\delta_0$, which we obtain by fitting Eq. (5) to the data in Fig. 3. The value $\phi + 2\delta_0 = -2.4$ rad yields a very good fit to the data.

As mentioned earlier, ϕ represents the sign of matrix elements, and it can take values of 0 or π. Apart from this discrete phase or sign ambiguity of 0 or π, we can obtain the quantity δ_0, which relates to the absolute timing of the attosecond pulse train. The 0 or π phase ambiguity can be easily removed using either of the two methods discussed below.

One method to establish whether $\phi = 0$ or $\phi = \pi$ is appropriate for the 2p Floquet state under consideration is to use TDSE simulations. These simulations establish that the phase ϕ in this situation is zero [16]. The other method to establish the value of ϕ is based on the fact that only one of these options leads to a physically justifiable answer for the time of birth of attosecond bursts. Using the possibility $\phi = \pi$, we can fit Eq. (5) to the data and obtain δ_0 as 0.37 rad. This corresponds to a XUV burst occurring 150 as before the peak of the IR field, which implies a 15th harmonic short-trajectory return phase of 160° relative to the negative peak of the IR field.

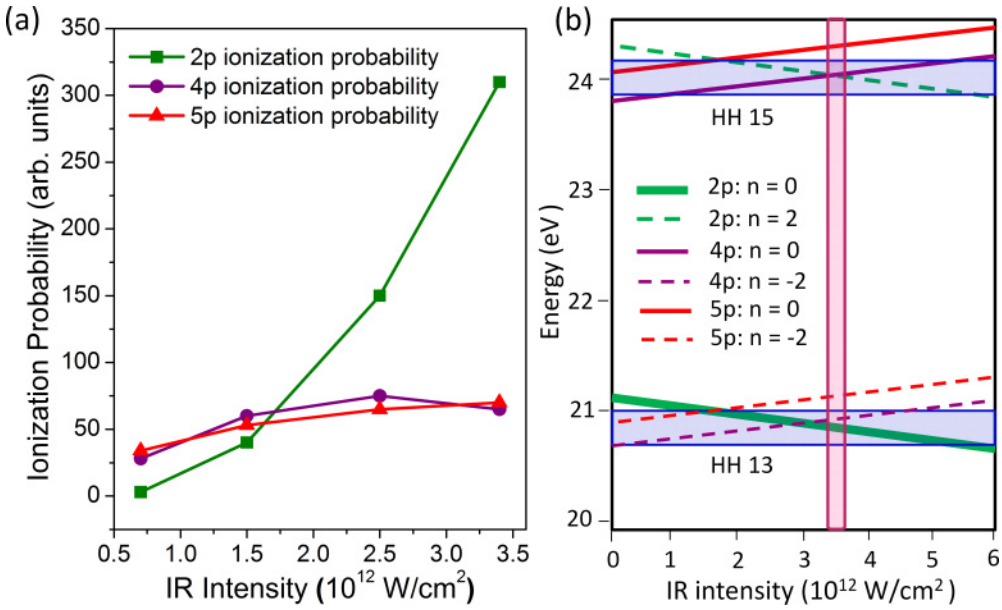

FIG. 4. (Color online) (a) Calculated ionization probability from the XUV excited $2p$, $4p$, and $5p$ states as a function of IR intensity. The $2p$ mediated ionization pathway dominates at high intensity and hence determines the phase of 2ω oscillations. (b) A schematic of the evolution of the $2p$, $4p$, and $5p$ Floquet blocks with IR intensity. Thicker lines represent a higher-absorption cross section. The horizontal blue boxes represent the harmonics. The vertical rectangle indicates the IR intensity regime used in our experiment.

A simple calculation of classical trajectories for harmonic emission [20] easily rules out this result as too short of a return time for the harmonics under consideration.

Using the second option, i.e., $\phi = 0$, we obtain a value of $\delta_0 = -1.2$ rad, which corresponds to an APT time of birth of 500 as after the peak of the driver electric field. This burst timing corresponds to the 15th harmonic short-trajectory return at 250° phase relative to the negative peak of the IR field. As shown in Fig. 5, this agrees well with the single-atom prediction for timing of near-cutoff harmonics in Xe gas being driven at 6×10^{13} W cm^{-2}. Furthermore, our measurement of the XUV burst timing relative to the IR field is also in qualitative agreement with the experimental results reported in Ref. [12].

From the above discussion it is clear that, in APT + IR pump-probe experiments, interferences between XUV transitions are determined by both the phases of light fields and quantum phases of transitions to laser-dressed resonances. The dynamics under these conditions cannot be fully captured by a classical cross correlation between light fields. However, the Floquet formalism provides a convenient approach for modeling the excitation to laser-dressed resonances. Though we have used an XUV spectrum with only two dominant harmonics in our experiment, this technique of extracting the timing can be applied to more general APTs consisting of many harmonics. In cases where harmonics beyond the 15th harmonic are present, the direct transitions to the continuum will increase the DC level of the ionization signal. Even if the background ionization level increases by an order of magnitude, by appropriate Fourier filtering, it should be possible to extract the few percent oscillations in the ionization signal, and hence the timing information can be extracted. In the case of isolated attosecond pulses, the broad, continuous spectrum of such pulses can create a complicated mixture of different Floquet states, which can make the measurement and analysis quite difficult. Hence, an important limitation of our technique is that it may not be applicable to isolated attosecond pulses.

In conclusion, we have obtained the time of birth of attosecond bursts produced by high-order-harmonic generation using the ionization of a laser-dressed helium atom as

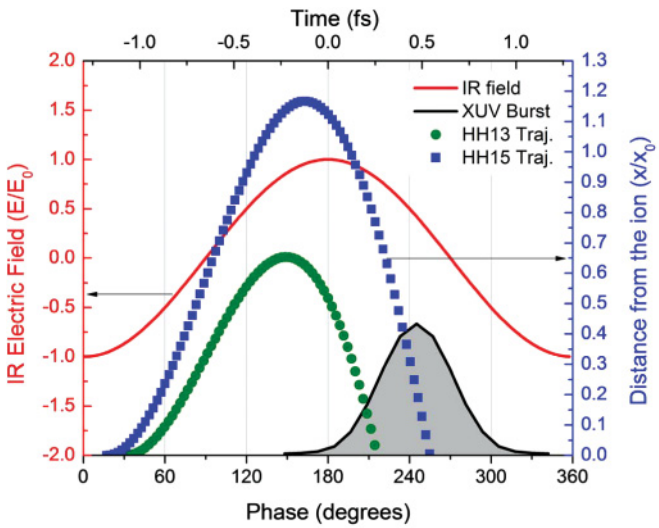

FIG. 5. (Color online) Classical short trajectories of the electron for the 13th and 15th harmonic generation in Xe at a laser intensity of 6×10^{13} W cm^{-2}. The electron excursion and electric-field amplitudes are $x_0 = 5.44$ a.u. and $E_0 = 0.18$ a.u. Note that the phases are measured from the negative peak of the IR field. The recollision phase for the 15th harmonic is thus 250°. The timing of a XUV burst corresponding to our harmonics is 500 as relative to the positive peak of IR field.

a measurement probe. The ion-yield signal, as a function of time delay, directly provides the absolute timing of the attosecond bursts when a single Floquet state dominates the ionization. The experimental knowledge of attosecond burst timing can be useful in many experiments of current interest where the result of an XUV-IR induced process critically depends on the absolute timing between the two fields. For example, it can be useful in obtaining deeper insight into processes like control of electron localization in molecular dissociation where the phase of the IR field at the time of excitation by the XUV field sets the initial conditions. In experiments which use high-order-harmonic generation to probe molecular structure and dynamics, the time of birth of attosecond bursts can help data analysis and interpretation by providing additional experimental constraints. In general, photoexcitation or photoionization with XUV pulse trains in the presence of strong laser fields involves multipath interferences whose result is determined by the quantum phase difference between paths as well as the absolute time delay between the XUV and IR fields. The knowledge of absolute XUV timing from measurements in helium can be used to obtain quantum phase differences between excitation or ionization channels in molecules, leading to quantum control schemes in the XUV regime.

This work was supported by the National Science Foundation (NSF) under Contract No. PHY-0955274.

[1] F. Krausz and M. Ivanov, Rev. Mod. Phys. **81**, 163 (2009).
[2] D. Shafir, Y. Mairesse, D. M. Villeneuve, P. B. Corkum, and N. Dudovich, Nat. Phys. **5**, 412 (2009).
[3] A. D. Shiner, B. E. Schmidt, C. Trallero-Herrero, H. J. Worner, S. Patchkovskii, P. B. Corkum, J. C. Kieffer, F. Legare, and D. M. Villeneuve, Nat. Phys. **7**, 464 (2011).
[4] P. M. Paul, E. S. Toma, P. Breger, G. Mullot, F. Auge, P. Balcou, H. G. Muller, and P. Agostini, Science **292**, 1689 (2001).
[5] S. Gilbertson, S. D. Khan, Y. Wu, M. Chini, and Z. H. Chang, Phys. Rev. Lett. **105**, 093902 (2010).
[6] A. S. Sandhu, E. Gagnon, A. Paul, I. Thomann, A. Lytle, T. Keep, M. M. Murnane, H. C. Kapteyn, and I. P. Christov, Phys. Rev. A **74**, 061803(R) (2006).
[7] E. Goulielmakis, M. Schultze, M. Hofstetter, V. S. Yakovlev, J. Gagnon, M. Uiberacker, A. L. Aquila, E. M. Gullikson, D. T. Attwood, R. Kienberger, F. Krausz, and U. Kleineberg, Science **320**, 1614 (2008).
[8] M. Hentschel, R. Kienberger, C. Spielmann, G. A. Reider, N. Milosevic, T. Brabec, P. Corkum, U. Heinzmann, M. Drescher, and F. Krausz, Nature (London) **414**, 509 (2001).
[9] P. Tzallas, D. Charalambidis, N. A. Papadogiannis, K. Witte, and G. D. Tsakiris, Nature (London) **426**, 267 (2003).
[10] H. G. Muller, Appl. Phys. B **74**, S17 (2002).
[11] L. C. Dinu, H. G. Muller, S. Kazamias, G. Mullot, F. Auge, P. Balcou, P. M. Paul, M. Kovacev, P. Breger, and P. Agostini, Phys. Rev. Lett. **91**, 063901 (2003).
[12] S. A. Aseyev, Y. Ni, L. J. Frasinski, H. G. Muller, and M. J. J. Vrakking, Phys. Rev. Lett. **91**, 223902 (2003).
[13] N. Shivaram, A. Roberts, L. Xu, and A. Sandhu, Opt. Lett. **35**, 3312 (2010).
[14] N. Shivaram, H. Timmers, X. M. Tong, and A. Sandhu, Phys. Rev. Lett. **108**, 193002 (2012).
[15] X. M. Tong, P. Ranitovic, C. L. Cocke, and N. Toshima, Phys. Rev. A **81**, 021404 (2010).
[16] X. M. Tong and N. Toshima, Phys. Rev. A **81**, 043429 (2010).
[17] S. I. Chu and D. A. Telnov, Phys. Rep. **390**, 1 (2004).
[18] P. Johnsson, J. Mauritsson, T. Remetter, A. L'Huillier, and K. J. Schafer, Phys. Rev. Lett. **99**, 233001 (2007).
[19] X. M. Tong and N. Toshima, Phys. Rev. A **81**, 063403 (2010).
[20] P. B. Corkum, Phys. Rev. Lett. **71**, 1994 (1993).